

Two-Dimensional Floquet Stability Analysis of the Flow Produced by an Oscillating Circular Cylinder in Quiescent Fluid

J. R. Elston¹, J. Sheridan¹ and H. M. Blackburn²

¹Department of Mechanical Engineering, Monash University, Victoria, 3800 AUSTRALIA

²CSIRO Division of Building, Construction & Engineering, PO Box 56, Highett, Victoria, 3190 AUSTRALIA

Email Contact: John.Elston@eng.monash.edu.au

Abstract

The two-dimensional symmetry breaking transition, from an initially time-periodic streaming flow produced by a circular cylinder oscillating in quiescent fluid at a low amplitude and frequency of oscillation, is examined using Floquet stability analysis. In experimental visualisations it has been observed that a number of distinct flow structures arise when the flow becomes unstable and the initial symmetry about the axis of oscillation (the reflection symmetry) is broken. Using Floquet analysis, two distinct symmetry breaking instabilities have been observed in the form of bifurcations to either a separate time-periodic solution or to a quasi-periodic solution (Neimark–Sacker bifurcation). These bifurcations correspond to the loss of either periodicity and/or reflection symmetry observed in experiments. Neutral stability curves and vorticity contours of the unstable modes are presented for values of the dimensionless oscillation amplitude (Keulegan–Carpenter number, KC), $KC < 10$ and frequency (Stokes number, β), $\beta < 100$.

Introduction

Two dimensionless control parameters determine the state of this flow. These are the Keulegan–Carpenter number $KC = 2\pi a/D$ and the Stokes number $\beta = fD^2/\nu$, where a is the amplitude of motion, D is the cylinder diameter and f is the frequency of oscillation. The visual observations of Honji (1981) and Tatsuno & Bearman (1990) identified a number of unique flow structures present in the wake for different combinations of KC and β . These structures were further classified into eight separate regimes by Tatsuno & Bearman (1990) on the basis of the two-dimensional flow structures observed and the presence of a three-dimensional instability along the cylinder span. Two-dimensional numerical simulations of these phenomena by Iliadis & Anagnostopoulos (1998) using a finite element method have obtained transition values slightly higher than those obtained by Tatsuno & Bearman (1990). Application of a spectral element method by Elston, Sheridan & Blackburn (2001) yielded results which more closely matched the known experimental values. In that study the location of the three-dimensional transition was obtained using Floquet analysis, while the two-dimensional transition locations were obtained using a combination of direct numerical simulation (DNS) and post-processing of the velocity fields at each time step to examine the symmetry of the velocity fields about the axis of oscillation. In the present work, attention is focused on the two-dimensional transition using Floquet stability analysis, and a number of new features emerge.

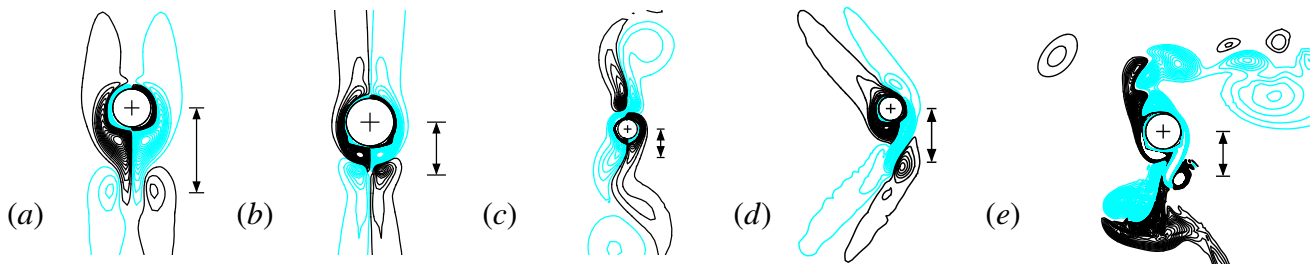


Figure 1: Close up of the two-dimensional DNS vorticity contours for the flow produced by a cylinder in vertical oscillation in Regimes A, B, C, D and E (regime labelling convention as defined in Tatsuno & Bearman (1990)). Also shown is the peak-to-peak amplitude of oscillation. (a) Regime A, $\beta = 12.5$ $KC = 7.0$; (b) Regime B, $\beta = 100.0$ $KC = 3.5$; (c) Regime C, $\beta = 40.0$ $KC = 5.0$; (d) Regime D, $\beta = 13.5$ $KC = 7.0$; (e) Regime E, $\beta = 100$ $KC = 4.0$. Cyan vorticity contours represent negative vorticity and black represents positive vorticity.

As the controlling parameters, KC and β , are increased and the wake undergoes the first two-dimensional transitions from its initial time-periodic, symmetrical state, three distinct flow regimes have been observed experimentally. Figures 1(a) and (b) show vorticity contours of the induced flow along the oscillation axis before the two-dimensional transition has occurred. The flow of these regimes, denoted A and B by Tatsuno & Bearman (1990), is periodic with the cylinder's oscillation. The flows of regimes C, D and E, shown in figure 1 (c-e), all exhibit breakage of the reflection symmetry about the oscillation axis. In regime D, figure 1(d), the induced flow direction has deviated from its previous course along the oscillation axis although the overall pattern retains a symmetry about the horizontal axis and the flow remains synchronised with the oscillation. The deviation is due to asymmetrical vortex pairs being formed on the top and bottom sides of the cylinder over a period of motion. However, these are not shed into the streaming flow as discrete vortices. In regime C, figure 1(c), large vortices form along the axis of oscillation and are shed as discrete vortices, creating a shedding pattern resembling a Kármán vortex street, with one major exception: the rotational direction of the vortices is opposite to that found

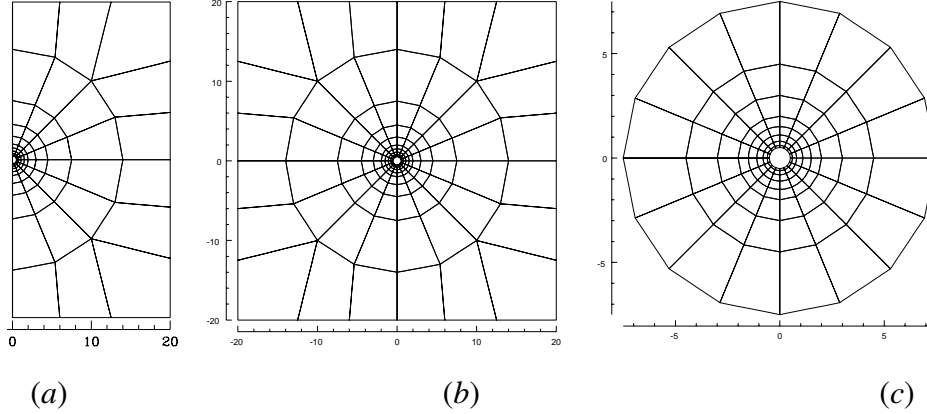


Figure 2: Spectral element domains used for computations. Shown is the 164 element $40D \times 40D$ domain, (b), used for Floquet stability calculations, the corresponding half-domain, (a), used to produce a symmetrical periodic base flow field and (c) a subsection used for determining outer boundary condition effects. The length scale is given in terms of the cylinder diameter D .

in the wake of a fixed circular cylinder; the flow is jet-like rather than wake-like. Vortices are shed with a new period, that is different from that of the oscillation period. Regime E, figure 1(e), produces similar effects to those occurring in regime D, however in this case the direction of the shed vortex pairs changes intermittently resulting in a loss of periodicity and symmetry about the oscillation axis.

In Floquet stability analysis a T -periodic flow, \mathbf{U} , is examined in conjunction with a perturbation, \mathbf{u}' , to the flow to determine whether the perturbation grows or decays in time. The evolution equations for the perturbation flow are the Navier–Stokes equations linearised about the T -periodic base flow. Perturbation solutions, \mathbf{u}' , can be written as a sum of components $\tilde{\mathbf{u}}(t) \exp \sigma t$ where $\tilde{\mathbf{u}}(t)$ are the T -periodic Floquet modes. Equivalent to the Floquet exponents σ are the Floquet multipliers μ , where $\mu = \exp \sigma T$. In the results presented here we use Floquet stability analysis to obtain the locus, in (KC, β) control space, of the two-dimensional symmetry breaking transition.

Computational Methodology

In the present implementation the periodic flow to be tested for stability (the ‘base flow’) is obtained using DNS. The DNS employed a spectral element spatial discretisation to solve the two-dimensional incompressible Navier–Stokes equations in an accelerating reference frame attached to the cylinder (Blackburn & Henderson 1999). To enforce the symmetry about the axis of the cylinder oscillation for the flow to be tested (the base flow), the domain used for the Floquet analysis was cut in half as seen in figure 2 (a) and (b). Along the vertical (y) side of the half domain the boundary conditions were set as $u = 0$ and $\partial v / \partial n = 0$ with a high-order pressure boundary condition. This simulation was run until a periodic base flow was obtained, at which point 64 field dumps, equi-spaced in time, were created over one period. These field dumps were subsequently projected onto the full domain, Figure 2(b), and used in the Floquet analysis as the base flow via Fourier series interpolation to reconstruct the periodic flow fields at each time step.

The linear stability of the symmetrical periodic base flow to infinitesimal perturbations was then calculated using Floquet stability analysis. In this technique the evolution of a system governed by the linearised Navier–Stokes equations is examined every time T , where T is the base flow period, to extract the leading eigenpairs of the evolving perturbation, $\mathbf{u}'(x, y, t)$, subject to the forcing of the periodic base flow, $\mathbf{U}(x, y, t)$, using a Krylov subspace method (Barkley & Henderson 1996).

The Floquet simulations were run on the full size domain with a Gauss–Lobatto–Legendre (GLL) polynomial interpolant order of 8 which was selected using the convergence tests in table 1(a). In these tests, the influence of interpolant order was found to result in a variation of less than 0.1% over the range of orders tested. The polynomial order was subsequently chosen to be identical to that used to create the base flows; convergence results for the base flow can be found in Elston et al. (2001). Convergence tests to determine an appropriate domain size found that the distance to the outer boundary slightly altered the magnitude of the Floquet multipliers due to the corresponding change in the base flow. The chosen domain size, $40D \times 40D$, reflects the average domain size used in the experiments of Tatsuno & Bearman (1990) with which we are comparing results. To ascertain whether the impact of the outer boundary conditions did not unduly influence our results the base flow was projected onto a smaller sub-domain, Figure 2(c), and the stability analysis was run on this smaller domain at $\beta=100.0$, $KC=3.65$. The Floquet multiplier was found to vary by less than 0.3% as a result of this and we conclude from this that the growth of a perturbation is determined by the dynamics close to the cylinder.

(a)	p	6	8	10	12
	$ \mu $	1.147180	1.147338	1.147052	1.146481
(b)	Domain Size	20×20	40×40	60×60	80×80
	$ \mu $	1.110241	1.147338	1.144826	1.142876

Table 1: Convergence results for Floquet multipliers at (a) different polynomial interpolant orders with a 40×40 domain. p is the order of the tensor-product interpolant function employed within each spectral element, (b) different domain sizes at $p = 8$. All simulations were conducted at $\beta = 100.0$ and $KC = 3.65$.

Results and Discussion

The locus of the critical Floquet multipliers for the first two-dimensional transition that occurred is shown in figure 3 as a function of KC and β . The location of the critical points closely matches the earlier experimental values obtained by Tatsuno & Bearman (1990) and the DNS results of the authors (Elston et al. 2001). Both real and complex critical Floquet multipliers were found to occur along the neutral stability curve, which denotes a break in the reflection symmetry. For low Stokes numbers (or alternatively, high Keulegan–Carpenter values) a real Floquet multiplier was the first to become unstable. In contrast, at low values of the Keulegan–Carpenter number (high Stokes numbers) a pair of complex Floquet multipliers was the first to become unstable. In the central region of figure 3, the real and complex branches of the unstable solutions are extremely close together. In this region the type of instability to emerge was found to be extremely sensitive to small changes in the controlling parameters, however, at no location were both real and complex solutions simultaneously unstable.

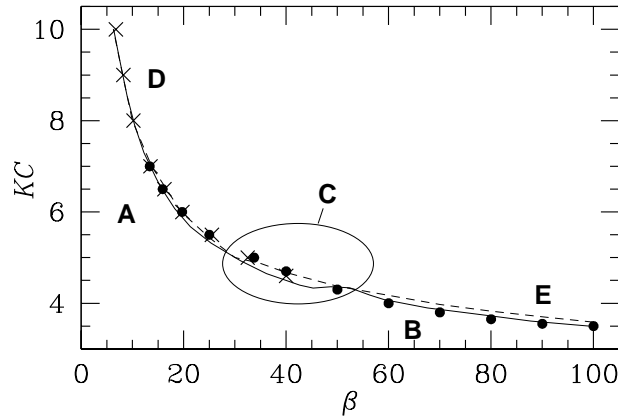


Figure 3: Critical Floquet multiplier dependence on KC and β . Shown are the results of Tatsuno & Bearman(1990), —, Two-dimensional DNS simulation results Elston et al. (2001), - -, unstable real Floquet multipliers, \times , and unstable complex Floquet multipliers, \bullet . Also indicated are the approximate locations of the regimes found by Tatsuno & Bearman, A, B, C, D & E.

The appearance of either type of multiplier appears to correlate with the type of symmetry breaking transition observed in experimental visualisations. Figure 4 shows the symmetric base flow and the growing real Floquet mode for a transition to regime D from A and a DNS result at a neighbouring location in regime D. In terms of vorticity the growing perturbation has an even reflection symmetry about the oscillation axis in comparison to the base flow which has an odd reflection symmetry. An important point to note here is that the combination of the growing perturbation and the base flow results in a flow which breaks the spatial symmetries observed about the oscillation axis, but is still synchronous with the base flow. The resultant DNS flow in figure 4(c) has clearly lost its reflection symmetry about the vertical (oscillation) axis and is also synchronised with the base flow.

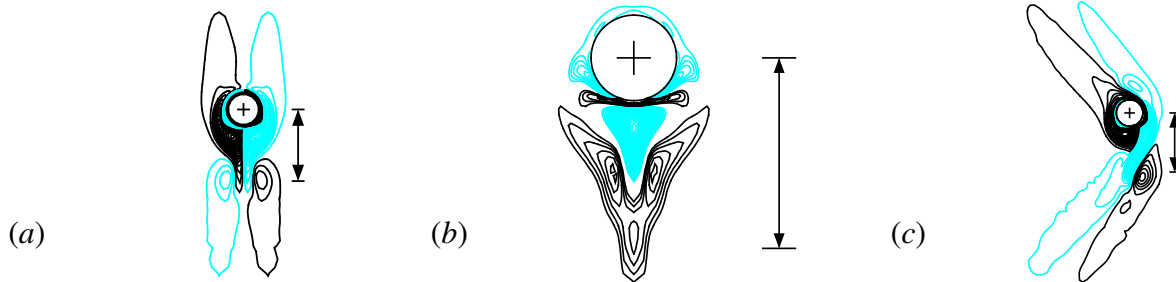


Figure 4: Vorticity contours for a transition across the neutral stability curve from regime A to D. Shown are: a) periodic base flow at $KC = 7.0$, $\beta = 13.5$; b) the leading real Floquet mode at $KC = 7.0$, $\beta = 13.5$; c) DNS results in regime D at $KC = 7.0$, $\beta = 15.0$.

The impact of an unstable complex Floquet multiplier is illustrated in Figure 5. The central section of figure 3, shown approximately as regime C, indicates a somewhat more involved transition is occurring. The flow in this regime has broken the reflection symmetry but is no longer periodic; instead it is quasi-periodic. Figure 5 illustrates a forced base flow, leading Floquet mode and DNS of flow in regime C. In this transition, which has a complex Floquet multiplier, the DNS vorticity contours, figure 5(c), far from the cylinder indicate the shedding of discrete vortices into the induced flow; a characteristic which was absent from the transition between regimes A and D (figure 4). However, near the cylinder the vorticity contours still resemble the contours of regime D, where the induced flow had broken reflection symmetry but the flow was still synchronised with the oscillation. The presence of a complex Floquet multiplier indicates the transition from a synchronous to a quasi-periodic state and this corresponds to the onset of shedding of discrete vortices into the induced flow. The bifurcation of forced periodic solutions into asymptotically quasi-periodic solutions are known as Neimark-Sacker bifurcations (Iooss & Joseph 1990).

Further progression along the neutral stability curve denoting the break in the two-dimensional reflection symmetry, towards high β values, encounters the transition from regime B to E as illustrated in figure 6. Experiments and DNS of the flow have shown that a

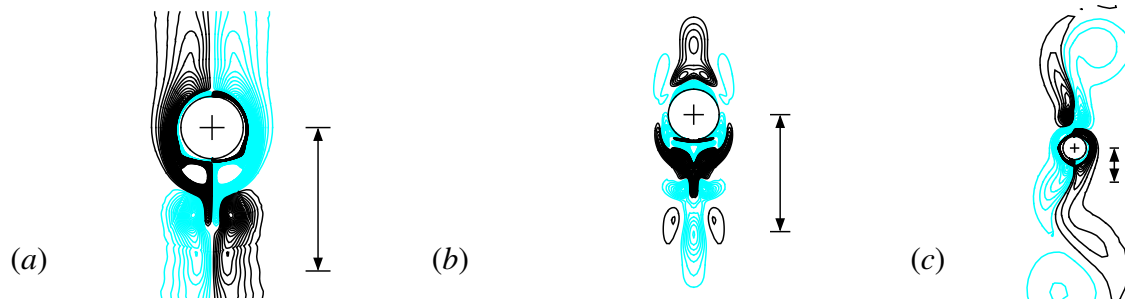


Figure 5: Vorticity contours for a transition across the critical transition curve from regime A to C. Shown are: a) periodic base flow at $KC = 4.60$, $\beta = 40.0$; b) one of the leading complex conjugate critical Floquet modes at $KC = 4.60$, $\beta = 40.0$; c) DNS results at $KC = 4.60$, $\beta = 44.2$.

transition to the flow of regime D initially emerges before the direction of the induced flow intermittently switches to either side of the oscillation axis, resulting in an aperiodic flow. As with the transition to regime C, an unstable complex Floquet multiplier indicates the transition to a quasi-periodic state and the onset of discrete vortex shedding. In this case the DNS of the flow indicates that the quasi-periodic state is only transient and the flow subsequently becomes aperiodic as the intermittent switching of the induced flow direction develops.

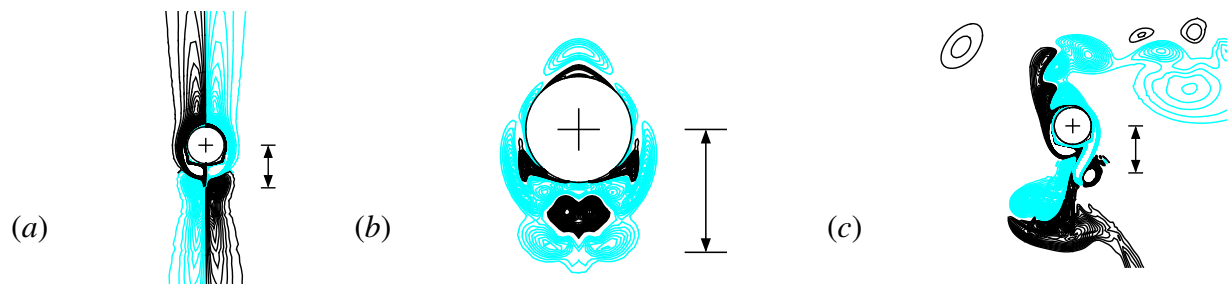


Figure 6: Vorticity contours for a transition across the neutral stability curve from regime B to E. Shown are: a) periodic base flow at $KC = 3.65$, $\beta = 90.0$; b) one of the leading complex conjugate Floquet modes at $KC = 3.65$, $\beta = 90.0$; c) DNS results in regime E at $KC = 3.65$, $\beta = 100.0$.

Conclusions

Two-dimensional Floquet stability analysis of symmetric periodic flows produced by an oscillating circular cylinder accurately matches the results obtained from experiments and DNS. The reflection symmetry about the oscillation axis is lost when the Floquet multiplier is greater than one, $|\mu| > 1$, while the presence of a non-zero imaginary component in the Floquet multiplier determines if the flow retains its synchronicity with the period of the forcing. As we traverse the neutral stability curve (which denotes the break in reflection symmetry) from the low β values towards high β values, the critical Floquet multiplier changes from real to complex. This change corresponds to a Neimark-Sacker bifurcation where a periodically forced flow bifurcates to a quasi-periodic state. The appearance of this bifurcation indicates the onset of the shedding of discrete vortices into the flow. Subsequent progression along the neutral stability curve towards even higher β values sees a change in the nature of the solutions observed using DNS from the quasi-periodic state of regime C to the chaotic (aperiodic) state evident in regime E.

Acknowledgements

We thank the Victorian and Australian Partnerships for Advanced Computing for their support.

References

- Barkley, D. & Henderson, R. D. (1996). Three-dimensional Floquet stability analysis of the wake of a circular cylinder, *J. Fluid Mech.* **322**: 215–241.
- Blackburn, H. M. & Henderson, R. D. (1999). A study of two-dimensional flow past an oscillating cylinder, *J. Fluid Mech.* **385**: 255–286.
- Elston, J. R., Sheridan, J. & Blackburn, H. M. (2001). The transition to three-dimensionality in the flow produced by an oscillating circular cylinder, *14th Australasian Fluid Mechanics Conference*, Adelaide University, Adelaide, Australia.
- Honji, H. (1981). Streaked flow around an oscillating cylinder, *J. Fluid Mech.* **107**: 509–520.
- Iliadis, G. & Anagnostopoulos, P. (1998). Viscous oscillatory flow around a circular cylinder at low Keulegan–Carpenter numbers and frequency parameters, *Intl J. Num. Meth. Fluids* **26**: 403–442.
- Iooss, G. & Joseph, D. D. (1990). *Elementary Stability and Bifurcation Theory*, 2nd edn, Springer-Verlag, Berlin.
- Tatsuno, M. & Bearman, P. W. (1990). A visual study of the flow around an oscillating circular cylinder at low Keulegan–Carpenter numbers and low Stokes numbers, *J. Fluid Mech.* **211**: 157–182.